HW VS SW SENSOR REDUNDANCY: FAULT DETECTION AND ISOLATION OBSERVER BASED APPROACHES FOR INERTIAL MEASUREMENT UNITS

Immacolata Notaro*, Marco Ariola, Egidio D'Amato*, Massimiliano Mattei***
***Dipartimento di Ingegneria Industriale e dell'Informazione, Seconda Univ. di Napoli,**
****Dipartimento di Ingegneria, Univ. di Napoli "Parthenope"**

Abstract

In this paper the use of different observer schemes based on Kalman Filtering for the detection and isolation of aircraft abrupt and incipient sensor faults on Inertial Measurement Units (IMUs) is discussed.

The possibility of using a dynamic 6DoF model of the aircraft is explored and compared with the use of a purely kinematic model. Both the possibilities are investigated assuming that two IMUs are available on board, and the analytic redundancy provided by the observers is used to vote the healthy one, when a fault occurs on accelerometers, gyros or magnetometers.

The proposed schemes are applied to simulated flight data of a General Aviation aircraft generated in the presence of disturbances and uncertainties.

Preliminary experimental results using two low cost IMUs are also shown for possible applications to improve safety and reliability of small Unmanned Air Vehicles.

1 Introduction

Sensor failures on aircraft may be critical for safety and costs. Sensor Fault Detection and Isolation (S-FDI) algorithmic strategies have been demonstrated to be a possible alternative to hardware redundancy, i.e. multiple independent hardware sensor channels, with a procedure to decide the healthy ones.

Analytical redundancy implies the use of mathematical relations to obtain the redundant measurements. Several techniques have been proposed in the literature to design state estimators for the solution of S-FDI problems [1-4], among which the best assessed are those based on parity space, observer-based methods, and approaches based on Kalman filter and on H_2 or H-infinity theory [5].

A Dedicated Observer Scheme (DOS) assumes a bank of observers where each of them is driven by a different output. In the event of a fault, the corresponding observer will produce inaccurate estimates and therefore fault detection and isolation is made possible [7].

A Generalized Observer Scheme (GOS), as the DOS, makes use of a bank of observers where each observer is driven by all outputs except one. In this way, when an output is faulty, the estimates of all the observer except one turn out to be inaccurate [8].

Both DOS and GOS can be used with Luenberger asymptotic state observers, Kalman Filters, Unknown Input Observers, or any other kind of state or output observer. Both of them require a decision making system to evaluate when the fault can be detected and isolated on the basis of the observer estimates.

An alternative to DOS or GOS bank of observers is a unique observer with an enlarged set of dynamics specialized to detect and isolate different kind of faults. In this paper we propose the use of such a kind of observer for the detection and isolation of aircraft sensor faults modeled as step signals (*abrupt faults*) or ramp signals (*incipient faults*) added to the raw IMU measurements, i.e. accelerations, angular rates, and magnetic field, provided by accelerometers, gyros, and magnetometers respectively.

The possibility of using a dynamic 6DoF dynamic model of the aircraft (type#1 observer) is explored and compared with the use of a purely kinematic model (type#2 observer). Both the possibilities are investigated assuming that two IMUs are available on board. In fact the main practical objective of the paper is to demonstrate the potential use of the S-FDI observers in the presence of IMU duplex hardware redundancy to allow fault detection and isolation, considering that a pure hardware redundancy scheme would require at least three different IMUs (triplex configuration).

The aircraft state space model is augmented with a bank of first order filters, one for each variable subject to possible faults. Indeed, in the ideal case of absence of model uncertainties, external disturbances and sensor faults, the additional dynamics are never excited. On the other hand, transients and/or steady state values of the additional state variables allows to detect and isolate faults if they occur.

Among the possible techniques to design observers, the use of the Unscented Kalman Filter technique [9] in the discrete time domain is explored considering that it can provide near-optimality against Gaussian noise and disturbances.

The proposed schemes are both applied to simulated data of a General Aviation aircraft. The observer based purely kinematic equations of motion is also tested on low cost IMUs for small UAVs for which safety and reliability becomes more and more important in view of massive civil applications.

The paper is organized as follows. The problem statement and the mathematical models adopted for the observers are illustrated in Section 2. Section 3 shows the residual generation schemes, i.e. the structure of the observer equipped with additional dynamics to generate the so-called residual variables. A possible decision making logic to declare the fault detection and isolation is also illustrated in this section. Simulation results in the presence of model uncertainties, sensor noise and wind turbulence and gusts on a general aviation aircraft are discussed in Section 4. Finally the proposed S-FDI observer based on kinematic equations (type #2 observer) is applied to experimental data collected from low cost IMUs typically used for small, mini or micro UAVs.

2 Problem Formulation and Open Loop Equations for the Nonlinear SFDI Observers

We assume that the aircraft is equipped with two IMUs, namely IMU-A and IMU-B, and that we have access to the raw signals coming from accelerometers, gyros, and magnetometers. If a fault occurs on one of the sensors of one of the IMUs (A or B), a comparison between the sensor output and the homologous from the other IMU allows to detect that a fault has occurred but leaves open the problem of which of the two IMUs is faulted.

To answer to this question a third IMU (triplex hardware redundancy scheme), or an analytical residual generation and evaluation systems tuned to identify the healthy IMU can be used.

We assume that only one fault at a time can occur, and that the fault can be modeled with a persistent signal added to the faulted sensor output. In particular abrupt faults are modeled with step functions and incipient faults with ramps although the proposed technique can work with other kind of persistent signals.

Two kind of observer based residual generation methods are compared.

Type #1 observer is based on the dynamic nonlinear rigid body 6 DoF model of the aircraft. This has the advantage that, in principle, it could be used to detect and isolate faults for one single IMU sensors without any hardware redundancy; on the other hand, the aircraft model has to be known with good accuracy in the whole operating envelope to avoid a high number of false alarms.

Type #2 observer is based on the nonlinear kinematic equations relating acceleration and angular rates to attitude. These equation are exactly known but there is the need of two IMUs to detect and isolate faults on all the nine sensors.

Both the observers have a common structure with a so-called open loop replication of the system dynamics, and a feedback

correction term based on the output estimation error.

We assume the following unified structure for the state space equations of the two models,

$$\dot{x} = f(x, u, w) \qquad (1)$$

$$y = h(x, u, w) + \mu \qquad (2)$$

Where x, u and y are the state, input and output vectors, w is the process noise vector, and μ is the measurement noise vector.

Denoting by $\hat{x}$ and $\hat{y}$ the estimates of the state and of the output, respectively, the observer equations comprehensive of the open loop dynamics and of the feedback correction term have the following structure

$$\dot{\hat{x}} = f(\hat{x}, u) + K(\hat{y} - y_m) \qquad (3)$$

$$\hat{y} = h(\hat{x}, u) \qquad (4)$$

where K is the so-called observer gain matrix.

2.1 Type#1 Observer Open Loop Equations

Type #1 observer is based on the nonlinear dynamic equations of a 6 Degree of Freedom (DoF) aircraft, that in our working example is a General Aviation aircraft. Using the symbols listed in Table 1, it is possible to write the equation of motion in the body axes in this form [10]

$$\begin{bmatrix} \dot{u} \\ \dot{v} \\ \dot{w} \end{bmatrix} = \frac{1}{m_{AC}} \left(- \begin{bmatrix} p \\ q \\ r \end{bmatrix} \times \begin{bmatrix} u \\ v \\ w \end{bmatrix} + F(V_B, \Omega, \Theta, \zeta, \delta, V_w) \right) \qquad (5)$$

$$\begin{bmatrix} \dot{p} \\ \dot{q} \\ \dot{r} \end{bmatrix} = I^{-1} \left(- \begin{bmatrix} p \\ q \\ r \end{bmatrix} \times I \begin{bmatrix} p \\ q \\ r \end{bmatrix} + M(V_B, \Omega, \Theta, \zeta, \delta, V_w) \right) \qquad (6)$$

$$\begin{bmatrix} \dot{\phi} \\ \dot{\theta} \\ \dot{\psi} \end{bmatrix} = \begin{bmatrix} 1 & sin\phi \cdot tan\theta & cos\phi \cdot tan\theta \\ 0 & cos\phi & -sin\phi \\ 0 & \frac{sin\phi}{cos\theta} & \frac{cos\phi}{cos\theta} \end{bmatrix} \begin{bmatrix} p \\ q \\ r \end{bmatrix} \qquad (7)$$

$$\begin{bmatrix} \dot{x}_E \\ \dot{y}_E \\ \dot{z}_E \end{bmatrix} = R_{BE}^{-1}(\phi, \theta, \psi) \begin{bmatrix} u \\ v \\ w \end{bmatrix} \qquad (8)$$

In (5) and (6), the force vector F and moment vector M, are the sum of three terms

$$F = F_A + F_T + F_G \qquad (9)$$

$$M = M_A + M_T \qquad (10)$$

where F_A and M_A are the aerodynamic forces and moments, F_T and M_T are the propulsive terms, and F_G is the gravity force.

$V_B = [u_B, v_B, w_B]^T$	Velocity vector in the body axes $[m/s]$
$\Omega = [p, q, r]^T$	Angular velocity vector in the body axes $[rad/s]$
$\Theta = [\phi, \theta, \psi]^T$	Attitude – Euler angles
$\zeta = [x_E, y_E, z_E]^T$	Position vector in inertial frame
$R_{BE}(\phi, \theta, \psi)$	Rotation matrix from inertial to body axes
$\delta = [\delta_e, \delta_a, \delta_r, \delta_f, \delta_{th}]^T$	Elevator, ailerons, rudder, flap deflection, and Throttle
$V_w = [u_W, v_w, w_w]^T$	Wind velocity vector in body axes $[m/s]$
m_{AC}	Aircraft mass $[kg]$
I	Aircraft inertia matrix $[kg \cdot m^2]$
α	Angle of attack
β	Angle of sideslip
$m = [m_x, m_y, m_z]^T$	Magnetic field in body axes $[Ga]$
$m_0 = [m_{0x}, m_{0y}, m_{0z}]^T$	Terrestrial magnetic field in inertial frame $[Ga]$
$a = [a_x, a_y, a_z]^T$	Acceleration vector in body axes $[m/s^2]$

Table 1 – List of symbols

Process disturbances to be taken into account for realistic simulations and performance evaluation of the proposed FDI scheme are atmospheric turbulence, for which we adopt a continuous Von Karman model, and wind gusts, that we model as a discrete wind gust [10].

In order to rewrite equation (5)-(8) in the compact form, given by (3) and (4), the following state, input and wind disturbance vectors are defined

$$x^{\#1} = [u, v, w, p, q, r, \phi, \theta, \psi, x_E, y_E, z_E]^T, \qquad (11)$$

$$u^{\#1} = [\delta_e, \delta_a, \delta_r, \delta_f, \delta_{th}]^T, \qquad (12)$$

$$w^{\#1} = [V_w^T, \dot{V}_w^T]^T. \qquad (13)$$

As for the measured outputs, since there are accelerometers, magnetometers, and rate gyros, the output vector is the following

$$y^{\#1} = [p, q, r, a_x, a_y, a_z, m_x, m_y, m_z]^T \qquad (14)$$

2.2 Type#2 Observer Open Loop Equations

Type #2 observer is oriented to attitude estimation, and is based on the nonlinear kinematic equation (7).

The following state vector can be assumed

$$x^{\#2} = [\phi, \theta, \psi]^T \qquad (15)$$

whereas inputs are measurements from gyros

$$u^{\#2} = [p_m, q_m, r_m]^T, \qquad (16)$$

process disturbance w is the gyro measurements noise, and the vector of measured outputs is the following

$$y^{\#2} = [a_x, a_y, a_z, m_x, m_y, m_z]^T \qquad (17)$$

which in steady state conditions and in the absence of perturbations to the terrestrial magnetic field vector m_0 are generated by the following output equations

$$\begin{bmatrix} a_x \\ a_y \\ a_z \end{bmatrix} = R_{BE}(\phi, \theta, \psi) \cdot \begin{bmatrix} 0 \\ 0 \\ g \end{bmatrix} \qquad (18)$$

$$\begin{bmatrix} m_x \\ m_y \\ m_z \end{bmatrix} = R_{BE}(\phi, \theta, \psi) \cdot \begin{bmatrix} m_{0x} \\ m_{0y} \\ m_{0z} \end{bmatrix} \qquad (19)$$

where g is the gravity acceleration.

3 The residual generation schemes

In the observer based schemes, FDI is typically achieved by combining a residual generator and a residual evaluation strategy which takes a decision on detection and isolation. The aim of the residual generation procedure is to compute quantitative indexes of the presence of faults called residuals.

If one single observer is used to generate residuals to detect and isolate different faults, an usual approach is to enlarge the system state with an additional vector of auxiliary variables, namely $\beta = [\beta_y^T, \beta_u^T]^T$, governed by first order dynamics, with time constants τ_y and τ_u respectively. These variables can be used to compensate for possible biases due to disturbances, measurement errors or uncertainties, modeled as additive contributions

to the outputs and the inputs in the classical estimation problems, but can be used as residuals in FDI schemes. Then the complete FDI observer scheme turns out to be that one shown in Fig. 1. This is governed by the following equations

$$\dot{\hat{x}} = f\left(\hat{x}, u + y_{\beta_u}\right) + K_1\left(\hat{y} - y_{\beta_y} - y_m\right) \qquad (20)$$

$$\dot{\beta}_y = -T_y\beta_y + K_2\left(\hat{y} - y_{\beta_y} - y_m\right) \qquad (21)$$

$$\dot{\beta}_u = -T_u\beta_u + K_3\left(\hat{y} - y_{\beta_y} - y_m\right) \qquad (22)$$

$$\hat{y} = h\left(\hat{x}, u + y_{\beta_u}\right) \qquad (23)$$

$$y_{\beta_y} = \beta_y \qquad (24)$$

$$y_{\beta_u} = \beta_u \qquad (25)$$

where T_y e T_u are diagonal matrices in which diagonal entries are equal to the inverse of the time constants τ_y and τ_u respectively.

The observer gain matrix $[K_1^T \quad K_2^T \quad K_3^T]^T$ can be computed in different ways [14]. In this paper we decided to convert all the differential equations into difference equations with a conversion to a sampled data system and to adopt an UKF algorithm.

With reference to the proposed observers, the two additional state vectors can be used as residuals, i.e. indicators of persistent sensor faults modelled as additive step or ramp signals also considering that, up to a certain tolerable value, they are used to compensate the unavoidable biases especially on gyros as in state estimation algorithms.

In ideal conditions, i.e. in the absence of disturbances, uncertainties and noise on sensors, and in fault-free conditions, the residuals should be small and deviate from zero only after the occurrence of the faults to which they are sensitive. However, in real world situations, there is the need to set up a residual evaluation strategy indicating whether the residuals can be considered small or not. This evaluation strategy involves the choice of positive thresholds and possible pre-filtering algorithms of the residuals (see Section 4).
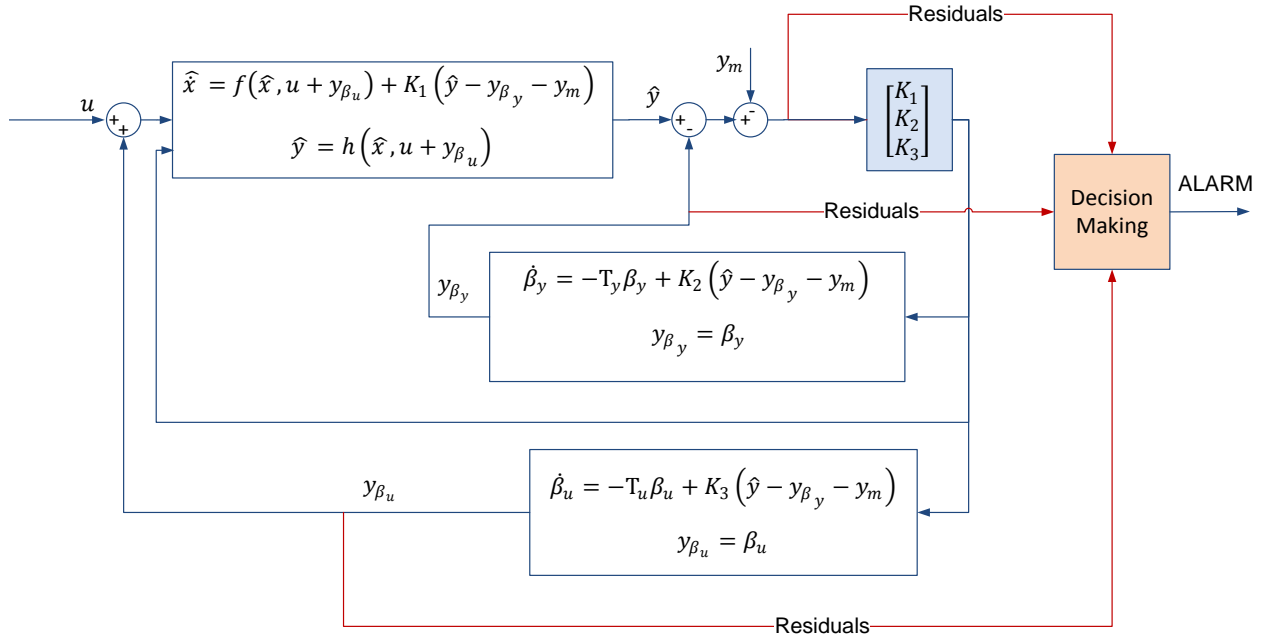
Fig. 1. The S-FDI observer scheme

3.1 Residuals Generation for Observer #1

In this case the input to the observer is the deflection of the control surfaces and the throttle. Since no possible bias is assumed on the measurement of the inputs, equations (20), (21), (23) and (24) can be used and the additive term β_u neglected. Assuming $\tau_y = +\infty$, i.e. integrator dynamics on the output residual, the observer equations have the following expression

$$\begin{bmatrix} \dot{\hat{x}} \\ \dot{\beta}_y \end{bmatrix} = \begin{bmatrix} f(\hat{x}, u) \\ 0 \end{bmatrix} + \begin{bmatrix} K_1 \\ K_2 \end{bmatrix} \left(\hat{y} - y_{\beta_y} - y_m \right) \qquad (26)$$

$$\begin{bmatrix} \hat{y} \\ y_{\beta_y} \end{bmatrix} = \begin{bmatrix} h(\hat{x}, u) \\ \beta_y \end{bmatrix} \qquad (27)$$

When a persistent fault on the i-th output variable occurs, only the i-th integrator starts charging, and the integrator state can be used as residual to detect and isolate such a fault.

3.2 Residual Generation for Observer #2

For type #2 observers we have a reduced set of three differential equations describing kinematics, and possible faults on nine different sensor (accelerometers, gyros, and magnetometers).

According to equations (7), gyro outputs are integrated to obtain attitude estimation, but such an estimation would suffer from large drifts due to integration in time of the gyro biases. For this reason also gyro biases are estimated on the basis of accelerometer and magnetometer measurements on a low frequency time scale (i.e. under the validity of assumptions for equations (18) and (19)). Equations (20), (22), (23) and (25) are then used as follows:

$$\begin{bmatrix} \dot{\hat{x}} \\ \dot{\beta}_u \end{bmatrix} = \begin{bmatrix} f(\hat{x}, u + y_{\beta_u}) \\ -\dfrac{1}{\tau_u} \beta_u \end{bmatrix} + \begin{bmatrix} K_1 \\ K_2 \end{bmatrix} (\hat{y} - y_m) \qquad (28)$$

$$\begin{bmatrix} \hat{y} \\ y_{\beta_u} \end{bmatrix} = \begin{bmatrix} h\left(\hat{x}, u + y_{\beta_u}\right) \\ \beta_u \end{bmatrix} \qquad (29)$$

It is worth to notice that, beside β_u, variables β_y and corresponding dynamics would be needed to have a sufficient number of residuals to detected and isolate faults on nine IMU measurements. However the kinematic model does not provide enough degrees of freedom for distinguishing among faults on different sensors. Therefore the possibility to distinguish among faults on gyros, accelerometers or magnetometers has to be left to proper decision making logics that make use of the β_u variables but also of the presence of two different IMUs on board.

3.3 Decision Making Logics

The first task of the decision making algorithm is to detect any significant changes in the residuals which can indicate the fault.

Assuming that we operate in the discrete time domain, if we denote by $r_i(k)$ the value of the i-th residual at the discrete time k, the goal can be achieved comparing the absolute value of residual $|r_i(k)|$ with a positive threshold σ_i.

The value of the threshold can be chosen on the basis of acceptable level of false and missed alarms probabilities [15] [16].

Residuals may need to be filtered before they are compared to thresholds. In fact, in our numerical case studies, we used some moving average means, moreover the result of a comparison between residuals and thresholds is consolidated only after a given number of consecutive samples.

A combination of residual evaluation and decision logics leads to the following algorithms for the two type of observers proposed in this paper.

Type#1 Observer FDI Algorithm
Each one of the two IMUs is equipped with a type#1 observer, namely observer#1-A and #1-B. The outputs of the two IMUs are compared to each other. If a significant difference is registered on one of the 9 raw measurements, the corresponding residuals from Observer #1-A and Observer #1-B are analyzed and a fault is declared on the sensor output for which the residual exceeds the threshold.

The faulted sensor is then excluded from the measurement system.

It is worth to notice that, with a more complex decision logic, the algorithm may work for more consecutive faults with multiple detections and isolations.

Type#2 Observer FDI Algorithm
Each one of the two IMUs (A and B) is equipped with a type#2 observer, namely observer#2-A and #2-B.
The following algorithm is repeated every discrete time step.

Step 1. First the norm of magnetometer measurements of each IMU is compared with the nominal expected value $\|m_0\|$. If a significant difference is registered, then a fault of a magnetometer is detected. To isolate on which axis the magnetometer gives a wrong output, a comparison between measurements A and B is made.

Step 2. If magnetometers are healthy, then the magnetometers outputs are compared with the magnetic field components estimates coming from the observers. If a difference is detected this is due to an error on the attitude estimation which in turn is due to an accelerometer fault, because gyro faults are compensated by the presence of β_u state variables. To isolate on which axis the accelerometers give a wrong output a comparison between measurements A and B is made.

Step 3. Finally if magnetometers and accelerometers are healthy, residuals $\beta_p, \beta_q, \beta_r$ are compared to selected thresholds to isolate a fault on p, q, or r gyro.

4 Numerical Simulations on a GA Aircraft

The two proposed FDI schemes have been tested in simulation in the Matlab-Simulink environment on a Technam P92 General Aviation aircraft simulation model. Several flight conditions have been considered including different manoeuvres and the presence of atmospheric turbulence, modelled with a continuous Von Karman model and a discrete wind gust.

In the following the results obtained with an elevator doublet manoeuvre (+5deg for 2s and -5deg for 2s) are illustrated with two different disturbance and uncertainty conditions. In fact, one of the drawbacks when using Type #1 observer is the sensitivity to uncertainties and disturbances.

Follows a description of the two conditions
S1 conditions - light atmospheric turbulence and no model uncertainties.
S2 conditions - moderate atmospheric turbulence, a discrete wind gust of amplitude with amplitude $V_{wind} = (3.5\ 3.5\ 3.0)\ m/s$ and length $(120\ 120\ 80)\ m$, uncertainties on stability and control derivatives.

For both conditions, measurement signals have been corrupted with noise, and faults have been simulated as additive signals to the outputs: step or ramp signals to simulate abrupt or incipient faults respectively.

Results with the following faults are shown:

a_x *sensor abrupt fault*: fault on a_x sensor modelled with a step signal of $2\ m/s^2$ centred at $t_f = 1s$;

p *sensor abrupt fault*: fault on p gyro sensor modelled as a step of $5 deg/s$ at $t_f = 1s$;

p *sensor incipient fault*: fault on p gyro simulated as a drift of $5\ deg/s^2$ starting at $t_f = 1s$

In all the plots, the residuals have been normalized in such a way that all the thresholds can be set to 1.

Results using type #1 observer

Fig. 2 shows residuals for S1 conditions in the presence of an a_x abrupt fault. The fault is detected and isolated after 0.55 s when the unit threshold is exceeded on the β_y residual corresponding to a_x.

Fig. 3 shows residuals in the case of p abrupt fault. The fault is detected and isolated after $0.55\ s$ when the unit threshold is exceeded on the β_y residual corresponding to p.

Fig. 4 shows the residuals for an a_x abrupt fault (same fault as for Fig. 2), but in the S2 conditions. In the presence of uncertainties and stronger disturbances, the situation is more confused as many residuals tend to reach the unit value. This makes the probability of false alarms higher and is the weak point of observer#1 FDI scheme. The detection and isolation time is $0.45\ s$.

Results using observer #2.

Fig. 5 and Fig. 7 and show results obtained with type#2 observer under S2 conditions for the same abrupt faults on a_x sensor and p sensor considered for type#1 observer. Magnetometers are assumed to be healthy in both simulations. Following the decision making logic describe in Section 3.3, this can be argued on the basis of a norm calculation filtered at low frequency (step 1).
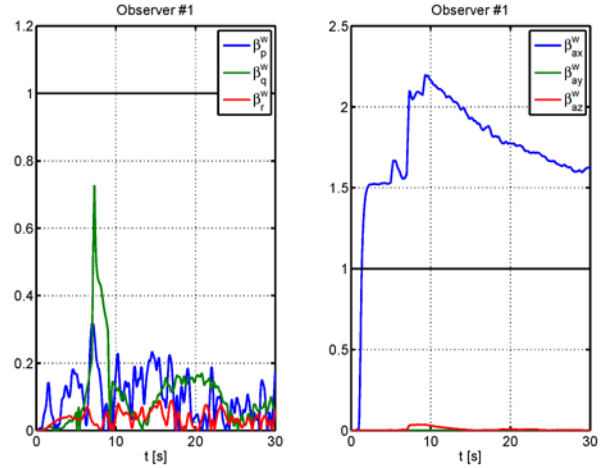
Fig. 2. Simulation in the presence of an abrupt fault on ax (S1 conditions). Weighted residuals on angular rates and accelerations calculated with type #1 observer.
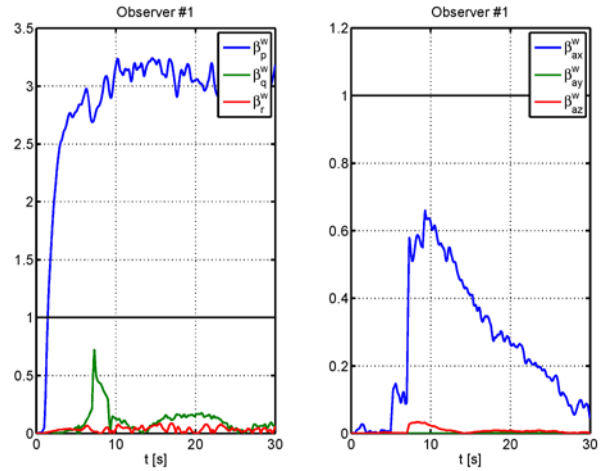
Fig. 3. Simulation in the presence of an abrupt fault on p (S1 conditions). Weighted residuals on angular rates and accelerations calculated with type #1 observer.
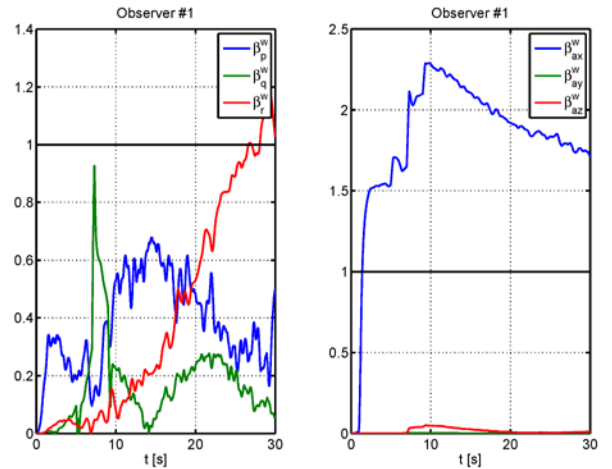
Fig. 4. Simulation in the presence of an abrupt fault on a_x (S2 conditions). Weighted residuals on angular rates and accelerations calculated with type #1 observer are shown.

For the simulation with a fault on a_x sensor (Fig. 5), looking at the difference between the estimated and the measured magnetometer output (Δ^w variables), we argue that a fault on IMU-B accelerometer holds. Then comparing the estimated acceleration from IMU-A and B, the fault on a_x IMU-B sensor is isolated after 0.11 s (step 2, see Fig. 6).
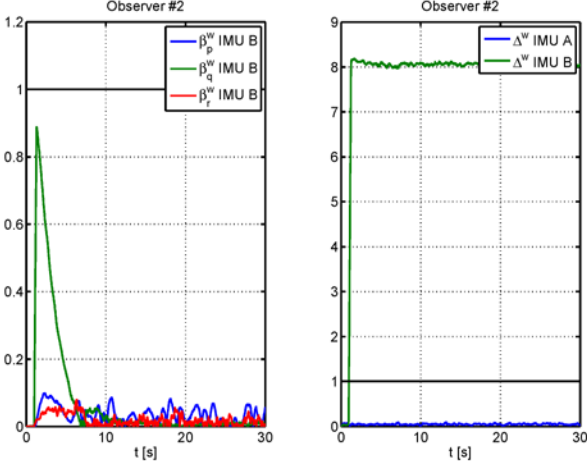

Fig. 5. Simulation in the presence of an abrupt fault on a_x (S1 condition). Weighted residuals of observer #2 . The residual linked to a_x is significantly larger than the others.
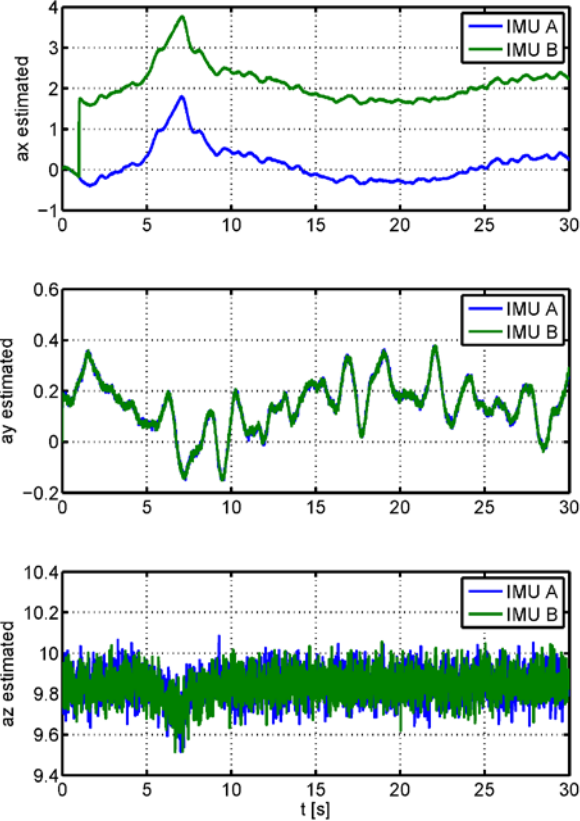
Fig. 6. Comparison between estimated acceleration from IMU-A and IMU-B. A fault on a_x is isolated due to the large difference between a_{xA} .and a_{xB}
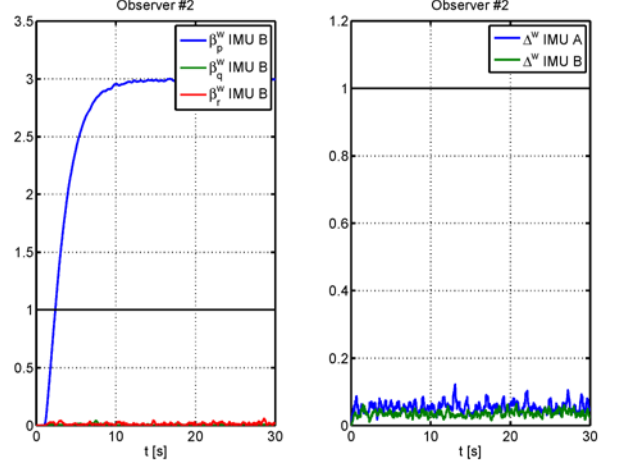
Fig. 7. Simulation in the presence of an abrupt fault on p (S1 condition). Weighted residuals of observer #2. The residual linked to p is significantly larger than the others.
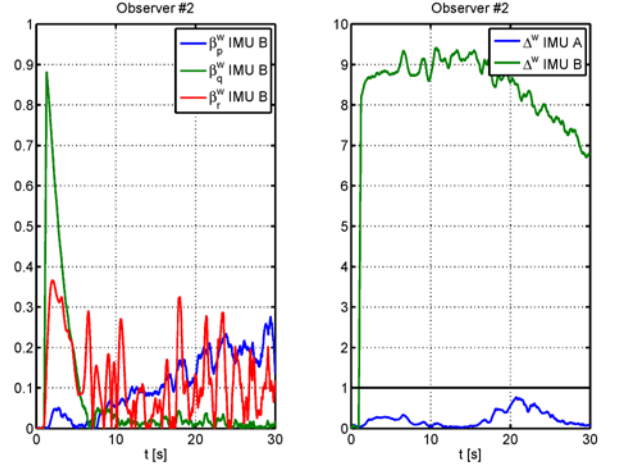
Fig. 8. Simulation in presence of an abrupt fault on a_x, consisting of a bias simulated as a step of $2\ m/s^2$ at $t_f = 1s$ (S2 condition).
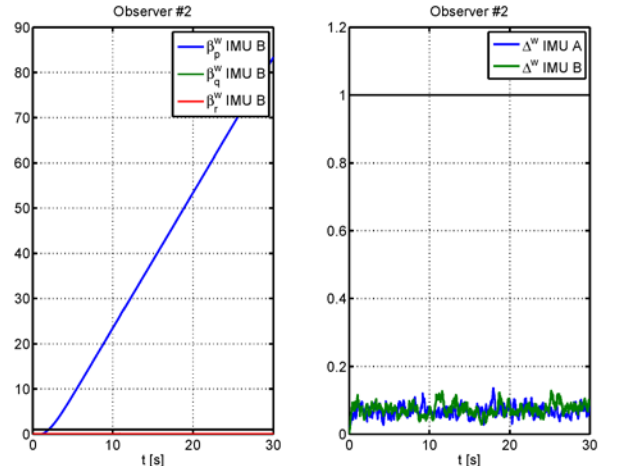

Fig. 9. Simulation in presence of an incipient fault on p, consisting of a drift of $5\ deg/s^2$ at $t_f = 1s$ (S2 condition).

For the simulation with a fault on p sensor (Fig. 7), looking at the difference between the

estimated and the measured magnetometer output (Δ^w variables for IMU-A and B), since they do not exceed threshold we argue that accelerometers are not faulted (step 2). Then looking at the β_p^w-IMU-B norm we isolate a fault on IMU-B x-axis gyro after 1.40 s (step 3).

The presence of uncertainties does not affect the observer performance as the kinematic equations do not depend on the dynamic model of the aircraft. As for the wind gusts and turbulence they introduce transients inducing an increase of the neglected terms in equation (17).

Fig. 8 shows results under S2 conditions and an abrupt fault on a_x, everything works as for Fig. 5, but Δ^w variables are all closer to the threshold due to transient accelerations induced by disturbances.

Fig. 9 shows the results under S2 conditions, for an incipient fault on p. β_p^w-IMU-B norm readily allows detection and isolation of the fault.

5 Preliminary results on low cost IMUs

Type#2 observer has been also tested on an experimental setup consisting of two low cost IMUs to test it for application to small UAVs for which safety and reliability becomes more and more important in view of massive civil applications. The setup is composed of two STM32F3Discovery development boards based on an ARM Cortex M4 family processor and three motion sensors: a 3-axis accelerometer, a 3 axis gyroscope and a 3-axis magnetometer. The two platforms were mounted on a data acquisition test-bed, to manually induce accelerations and rotations. The boards were synchronized at a sampling rate of 100Hz for sensor data acquisition.

In Fig. 10, β^w residuals and Δ^w variables for both IMUs are shown in the presence of experimental data and a simulated abrupt fault on a_x obtained adding a step to the acceleration measurement from IMU-B. The fault is detected by means of Δ^w norm. Then, as illustrated in Fig. 11, the isolation of the a_{xB} fault is achieved looking at the difference between homologous measurements from IMU-A and IMU-B.
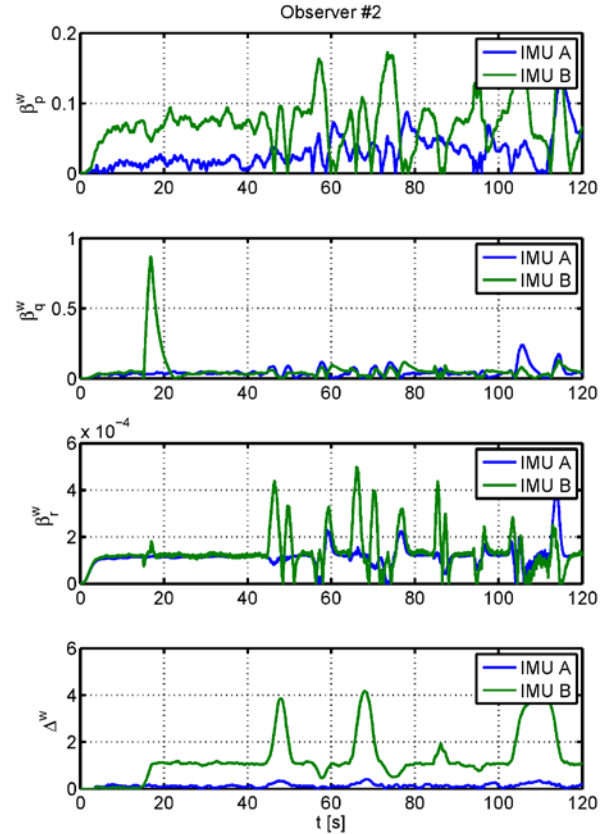

Fig. 10. Experimental data with simulated abrupt fault on a_x
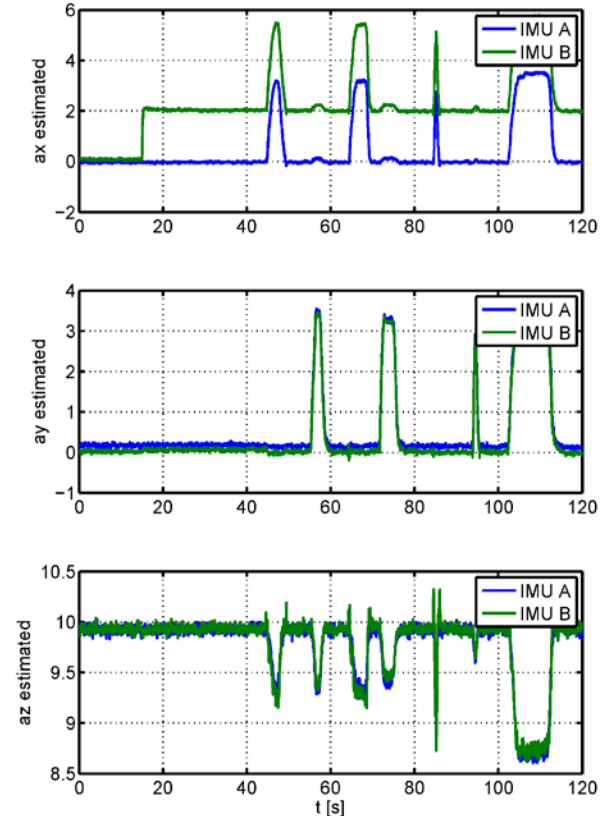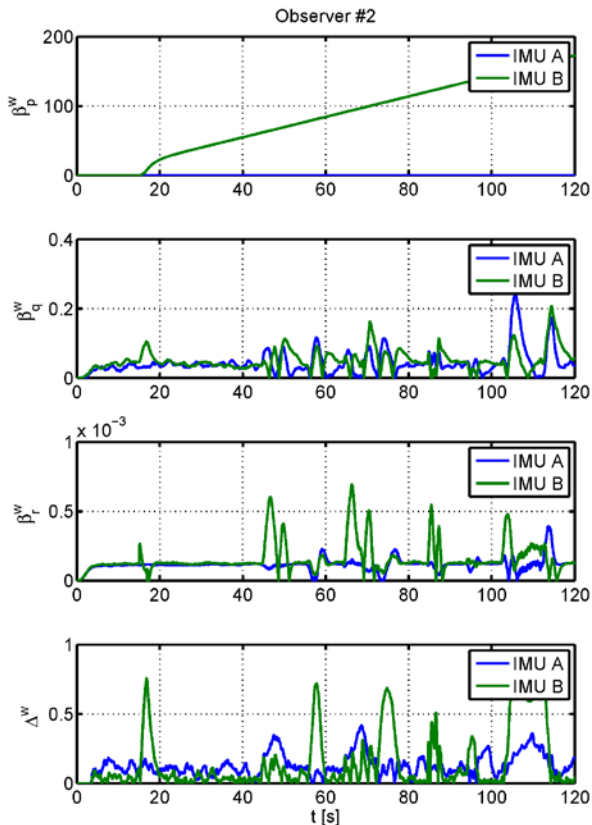

Fig. 11. Experimental data with simulated abrupt fault on a_x

Fig. 12. Experimental data with simulated incipient fault on p

6 References

[1] J. Chen and R. J. Patton. Robust Model-Based Fault Diagnosis for Dynamic Systems. *Kluwer Academic Publishers Norwell*, MA, USA, 1999.

[2] M. Basseville and I. V. Nikiforov. Detection of Abrupt Changes: Theory and Application. *Prentice Hall*, Englewood Cliffs, NJ, 1993.

[3] I. Hwang , S. Kim , Y. Kim and C. Seah. A survey of fault detection, isolation, and reconfiguration methods. *IEEE Trans. Control Syst. Technol.*, Vol. 18, No. 3, pp 636 -653, 2010

[4] I.Samy, I. Postlethwaite and Da-WeiGu. Survey and application of sensor fault detection and isolation schemes. *Control Engineering Practice* Vol. 19, pp 658–674, 2011

[5] M.Mattei, G.Paviglianiti and V.Scordamaglia. Nonlinear observers with H-infinity performance for sensor Fault Detection and Isolation: a Linear Matrix Inequality design procedure. *Control Engineering Practice*, Vol. 13, No. 10, pp 1271-1281, 2005.

[6] F. Amato, C. Cosentino, M.Mattei and G.Paviglianiti. A Direct/Functional Redundancy Scheme for Fault Detection and Isolation on an Aircraft. *Aerospace Science and Technology*, Vol. 10, Issue 4, pp 338-345, May 2006.

[7] R. N. Clark The dedicated observer approach to instrument failure detection. *Decision and Control*

including the Symposium on Adaptive Processes, 1979 18th IEEE Conference on, Vol.18, pp.237-241, Dec. 1979

[8] E. Kiyak, Ö. Çetin and A. Kahvecioglu. Aircraft sensor fault detection based on unknown input observers. *Aircraft Engineering and Aerospace Technology*, Vol. 80, No. 5, pp 545-548

[9] E. A. Wan and R. Van Der Merwe. The unscented Kalman filter for nonlinear estimation. *Adaptive Systems for Signal Processing, Communications, and Control Symposium 2000. AS-SPCC. The IEEE 2000*. pp 153-158, 2000.

[10] B. L. Stevens and F. L. Lewis. *Aircraft Control and Simulation*, 2nd edition, John Wiley & Sons, Inc, 2003.

[11] U.S. Military Specification MIL-F-8785C, 5 November 1980.

[12] D. G. Luenberger. Observers for multivariable systems. *Automatic Control, IEEE Transactions on.* Vol.11, No. 2, pp 190-197, 1966.

[13] N. Metni, J. M. Pflimlin, T. Hamel, and P. Soueres. Attitude and gyro bias estimation for a flying UAV. In *Intelligent Robots and Systems, 2005.(IROS 2005). 2005 IEEE/RSJ International Conference on.* pp 1114-1120, 2005.

[14] D. J. Simon. *Optimal State Estimation: Kalman, H Infinity, and Nonlinear Approaches*. 1st edition, Hoboken, N.J: Wiley-Interscience, 2006.

[15] M. Ariola, F. Corraro, M. Mattei, I. Notaro, and Sollazzo. An SFDI observer-based scheme for a general aviation aircraft. *Control and Fault-Tolerant Systems (SysTol), 2013 Conference on.* pp 152-157, 2013.

[16] M. Basseville On-board component fault detection and isolation using the statistical local approach. *Automatica*, Vol. 34, No. 11, pp 1391–1415, 1998.

7 Contact Author Email Address

mailto: massimiliano.mattei@unina2.it

Copyright Statement